

ADAPTATION OF MOTION SIMULATION TO THE REQUIREMENTS OF PILOT-IN-THE-LOOP STUDIES

ANPASSUNG DER BEWEGUNGSSIMULATION AN DIE ANFORDERUNGEN VON PILOT-IN-THE-LOOP

L. Fucke, R. Luckner

TU Berlin, Institut für Luft- und Raumfahrt, Marchstrasse 12, 10587 Berlin

OVERVIEW

This report gives a short overview on human motion perception and implications for ground-based motion simulation. Aspects of the implementation of the motion drive algorithm in the flight simulator of Zentrum für Flugsimulation Berlin (ZFB) are discussed. Subsequently experimental results on the simulator motion system's dynamic characteristics are presented and used to define goals for adapting the simulator motion system to the specific requirements of pilot-in-the-loop studies at Technical University Berlin. Adaptation methods and tools based on test data and a simulation model of the motion system are developed. Finally first results of the adaptation process as well as an outlook on follow-on work are given.

1. INTRODUCTION

Availability of ZFB's Full-Flight-Simulator as research instrument makes Technical University Berlin's facilities especially well suited for pilot-in-the-loop studies in which human motion perception is of high importance. A unique feature of the certified Level D flight simulator is its dual use capability for airline training and research purposes alike. So far this meant using the motion system during research operation in a set-up which has been optimized for the reproduction of motion cues essential for training operation. As pilot-in-the-loop studies conducted at the Flight Mechanics and Control group include flying the airplane outside the typical training envelope, such as during wake vortex encounter simulations, it was necessary to scrutinize motion system characteristics and develop approaches and tools to adapt the motion system to the particular demands of pilot-in-the-loop investigations.

In order to understand the objectives of motion simulation and the function of a motion platform, the basics of human motion perception need to be explained. As FIG 1 shows, motion perception uses a variety of sensory channels. Out of these channels a simulator motion system primarily stimulates the vestibular, tactile and proprioceptive systems.

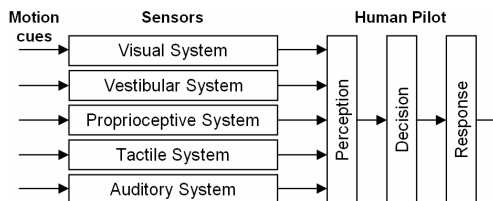


FIG 1. Perception and processing of motion cues (Ref.[3])

The capability of ground-based motion simulation to reproduce real flight motion is limited due to the restricted envelope of any motion platform. The motion system of the flight simulator at Technical University Berlin, as depicted in FIG 2, features a hydraulic six degree of freedom Stewart Platform, also called Hexapod. Excursion limits of a simulator platform are given in TABLE 1.

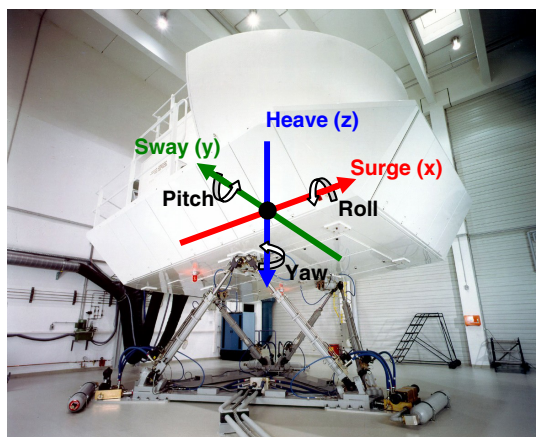


FIG 2. Hydraulic 6-degree of freedom (DOF) motion platform of the simulator at Zentrum für Flugsimulation Berlin

Axis	Excursion	Velocity	Acceleration
Surge	+/- 1.4m	+/- 0.7m/s	+/- 0.8g
Sway	+/- 1.2m	+/- 0.7m/s	+/- 0.8g
Heave	+/- 0.9m	+/- 0.6m/s	+/- 1.0g
Roll	+/- 28°	+/- 25°/s	+/- 250°/s ²
Pitch	+/- 34°	+/- 25°/s	+/- 250°/s ²
Yaw	+/- 37°	+/- 25°/s	+/- 250°/s ²

TABLE 1. Limitations of the simulator motion system

In addition to actuator travel, motion capabilities are also limited by maximum actuator velocity and force, resulting in platform velocity and acceleration constraints. The many restrictions of ground-based motion simulation make it necessary to focus on providing the pilot with vestibular motion cues instead of attempting a full reproduction of aircraft motion.

2. MOTION SIMULATION

2.1. Vestibular Motion Perception

The human vestibular apparatus is capable of determining body orientation and acceleration. It comprises a pair of vestibular organs situated in the inner ears. The otoliths and semicircular channels serve as actual motion sensors for linear and rotary motion respectively. Body orientation is established based mainly on the components of steady-state acceleration, i.e. the direction of the gravity vector. In linear as well as rotary axes perceptual thresholds exist. Linear accelerations are perceived above a rather slim threshold of about 0.01g. Thresholds in rotary perception are in the order of 3deg/s about roll axis, 2.5deg/s about pitch and 1deg/s about yaw axis. The semicircular channels of the vestibular system, which sense rotary motion, show dynamic characteristics of an integrator on the frequency range relevant for piloting an aircraft. Stimulation response therefore is proportional to angular velocity instead of acceleration, effectively making the semicircular channels angular rate sensors. It is also of importance that perceptual thresholds will increase in the presence of multiple stimuli, such as during superposition of linear and rotary cues or added visual and auditory stimuli. Consequently threshold values to be observed in an actual simulated piloting task will be significantly higher than the ones stated above. To obtain more detailed information on human motion perception study of Ref. [1] and [2] is recommended.

2.2. Generation of Motion Cues

Based on the knowledge on human motion perception the motion system has to reproduce linear accelerations and angular velocities of the aircraft. Due to the limited excursion of the motion platform, only higher frequency motion can be realized. Thus a motion cueing algorithm primarily is a high-pass filter. However, in longitudinal and lateral direction, tilting of the simulator cabin can effect sensation of steady linear acceleration, as the vestibular system does not discern a gravity component from an additional acceleration. If so-called tilt-coordination is performed below rotary perceptual thresholds, the pilot will not sense any false pitch or roll cues. Integrating high-pass linear acceleration and low-pass tilt-coordination channel effectively yields a complementary filter for lateral and longitudinal acceleration. FIG 3 presents a schematic of the resulting motion cueing algorithm.

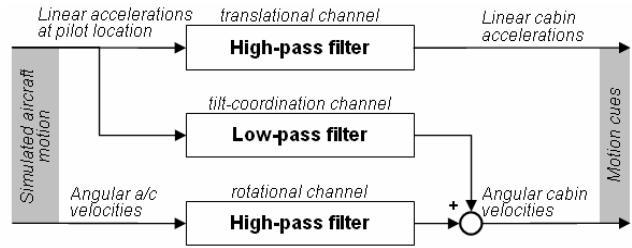


FIG 3. General structure of a motion cueing algorithm

Given this architecture of a motion cueing algorithm and the limitations of the motion system listed in TABLE 1, a dynamic envelope of the motion system, i.e. realizable acceleration (also velocity and displacement), can be concluded as a function of signal frequency. An envelope for lateral (sway) motion is depicted in FIG 4.

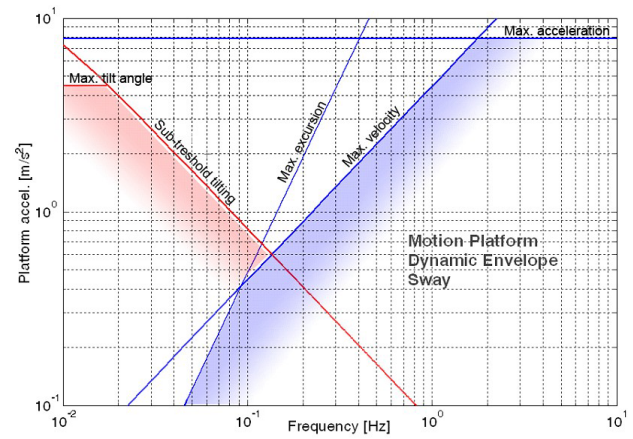


FIG 4: Typical dynamic capabilities of a Hexapod motion platform in lateral direction

The blue shaded area in the right of the plot is marking the translational capability of the system, limited to the top by maximum acceleration, to the left by maximum excursion for higher frequencies, by maximum velocity for lower frequencies. The red shaded area on the left is added by introducing tilt-coordination, i.e. it is missing in vertical axis. Tilt-coordination capabilities are limited by maximum tilt angle to the top and the angular velocity perceptual threshold to the right; in this case 3deg/s was used to compute the boundary. Full reproduction of real flight motion cues is possible in the shaded areas only; outside of the envelope motion cues have to be attenuated.

2.3. Nominal Research Configuration of the Motion System

The nominal research configuration described here, is a broadband motion cueing set-up, as it is suitable for pilot training. Structure of the cueing algorithm largely resembles the one presented in FIG 3. To obtain an effective attenuation of low-frequency motion 2nd and 3rd order high-pass filters are used in linear acceleration and angular rate channels respectively. Dropping the idea of ideal complementary filtering in longitudinal and lateral axes a 2nd order low-pass filter is employed in the tilt-coordination channel. FIG 5 presents the algorithm in more detail.

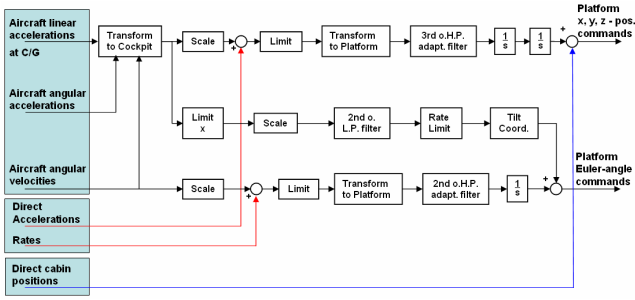


FIG 5. Detailed structure of the motion cueing algorithm (nominal research configuration)

Firstly accelerations at the pilot's seat are computed from the accelerations at the aircraft's center of gravity \underline{a}_{CG} , aircraft angular velocities $\underline{\omega}$ and the lever arm from center of gravity to the cockpit \underline{r}_{cpt} . The general expression to compute acceleration at the pilot's location is

$$(1) \quad \underline{a}_{cpt} = \underline{a}_{CG} + \underline{\omega} \times (\underline{\omega} \times \underline{r}_{cpt}) + \dot{\underline{\omega}} \times \underline{r}_{cpt}$$

As $r_{cpt,x} \gg r_{cpt,y}, r_{cpt,z}$, lever arm components in x- and y-direction are neglected, yielding

$$(2) \quad \begin{aligned} a_{cpt,x} &= a_{CG,x} - (q^2 + r^2)r_{cpt,x} \\ a_{cpt,y} &= a_{CG,y} + (pq + \dot{r})r_{cpt,y} \\ a_{cpt,z} &= a_{CG,z} + (pr - \dot{q})r_{cpt,z} \end{aligned}$$

After scaling, limiting and transformation into the motion platform's inertial frame the signals are passed through the high-pass filters. Integration of the filter output yields platform position and Euler-angle commands. Performing the filtering after transformation into the platform's inertial frame ensures accurate return of the platform to its neutral position. The longitudinal/lateral tilt-coordination channel also includes a rate limiter to keep tilt command below the perceptual thresholds. Additionally, direct cockpit acceleration and angular rate command channels, as well as a direct cabin position command channel is implemented to simulate special effects such as hard bumps during taxi.

On top of the classical washout filter design, the cueing algorithm features real-time adaptation of high-pass filter gains, making it a hybrid cueing filter. The filter gain K_a of the 3rd order acceleration filter of the form

$$(3) \quad H(s) = K_a \cdot \frac{s^3}{s^3 + K_v s^2 + K_p s + K_i}$$

is determined using a cost-function, weighting for example filter in- and output accelerations a_{in} and a_{out} , commanded platform velocity v_{out} and position p_{out} as well as deviation of the current filter gain K_a from initial value $K_{a0} = 1$.

$$(4) \quad K_a(s) = \frac{1}{s} \cdot G \cdot \begin{bmatrix} (a_{in}^2 - a_{out} a_{in})T - w_1 v_{out} \frac{1}{s} a_{in} T \dots \\ \dots - w_2 p_{out} \frac{1}{s^2} a_{in} T - (K_a - K_{a0})w_3 \end{bmatrix}$$

With $0 \leq K_a \leq 1$

In this quadratic cost function, T denotes the 3rd order transfer function

$$(5) \quad T(s) = \frac{s^3}{s^3 + K_v s^2 + K_p s + K_i}$$

whereas w_1 through w_3 are individually tunable weighting factors. Coefficient G represents a cost function derivative gain and determines rate of filter adaptation. Due to the shape of equations (4) and (5) the filter gain K_a varies with the input signal a_{in} (between 0 and 1). FIG 6 illustrates impact of magnitude and frequency of a harmonic acceleration input on mean value of the gain K_a .

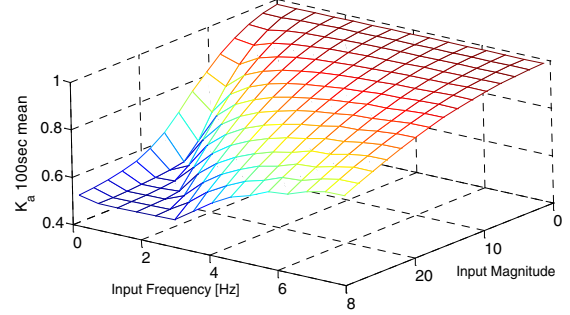


FIG 6: Impact of input magnitude and frequency on 100s-mean filter gain K_a (harmonic signal, weighting function and filter parameters see FIG 7)

Obviously high input magnitudes and low input frequencies result in low values of the gain K_a , meaning increased attenuation. This behavior is required as the motion platform's capabilities are limited for large magnitude/low frequency inputs. It has to be noted though that on-line variation of the filter gain introduces additional dynamics into the system which can eventually result in false motion cues. Generally real-time gain adaptation using a well-shaped cost function and optimized weighting factors enables optimized use of the platform envelope for a given task. FIG 7 compares frequency response of a filter of the above form using a constant gain $K_a = 1$, against a filter using real-time gain adaptation for different input magnitudes.

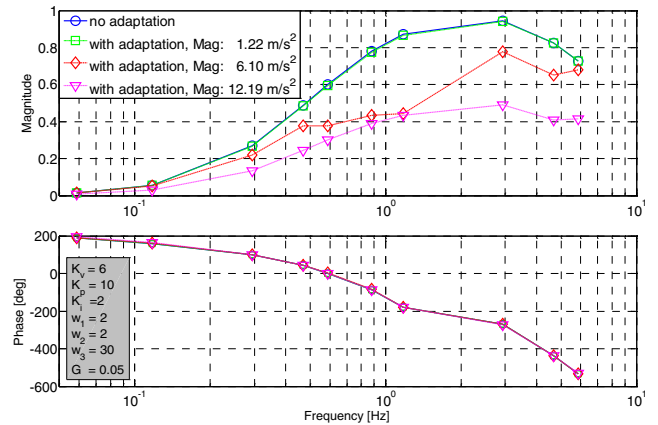


FIG 7. Effect of gain adaptation on characteristic of 3rd order high-pass motion filter

For small excitation magnitudes the adaptive gain filter shows identical magnitude as the constant gain filter. With increasing input magnitude the filter gain's dependency on input frequency and magnitude, pictured in FIG 6,

becomes clearly visible. As FIG 7 shows gain adaptation has no impact on phase behavior of the filter.

3. MOTION SYSTEM CHARACTERISTICS

In order to adapt the motion system to special research needs a detailed knowledge of architecture and characteristics of the system has to be developed. This includes experimental identification of dynamic response of the system as well as creating a simulation model and validating the model using the collected test data.

3.1. Measurement of Motion Response

3.1.1. Test Set-Up and Conduct

The motion cueing software is running on a dedicated motion computer, which is equipped with the necessary hardware for 2-way communication with the simulation host computer over a manufacturer proprietary data bus and digital/analog input/output cards to drive and monitor the hydraulic motion system. Monitoring hardware also includes a set of accelerometers mounted at the base of the motion platform. From accelerometer readings linear accelerations and angular rates at the geometric centroid of the actuator joint points are derived in the motion computer. Additionally, a 3-axis accelerometer has been installed under the captain's seat, to measure directly at the pilot's location. A/D conversion and transfer to the host computer for data recording is realized by a test interface computer ("Test Bench"). For synchronization of the accelerometer inputs with the test data a saw-tooth signal is generated in the simulation host and passed through the seat accelerometer signal path. Correlation of output and input synchronization signal yields the time delay on the signal path between host and test bench, drawn as dotted line in FIG 8. Pilot seat accelerometer data are corrected for that time delay during post-processing.

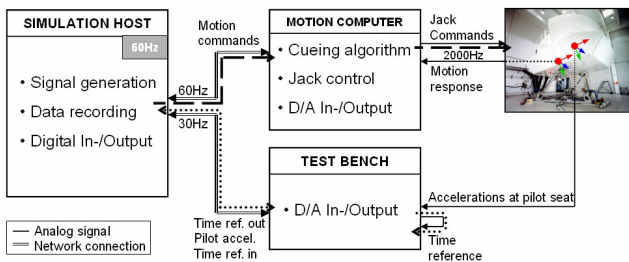


FIG 8. Test set-up for motion system identification

To determine the motion system describing functions harmonic excitation signals according to AGARD AR-144 (Ref. [4]) are generated in the simulation host code. The generated sine signals have discrete frequencies; each frequency is being held for a duration of $N = 1024$ samples. At the simulator host computer's sample rate of 60Hz that equals a time of $T = 1024 \cdot \frac{1}{60} s = 17.067s$ per excitation frequency. In the actual tests each frequency was held for 19s to establish a steady-state oscillation after changing frequencies. The signal frequencies are determined using

* Equivalent linear transfer function of a non-linear system; ratio of the Fourier-transforms of system output and sinusoidal input signal at fundamental frequency

the relationship

$$(6) f_i = \frac{k_i}{T}.$$

With

$$k_i = 1, 2, 5, 8, 10, 15, 20, 50, 80, 100,$$

which yields

$$k_i = 0.06\text{Hz}, 0.12\text{Hz}, 0.29\text{Hz}, 0.47\text{Hz}, 0.59\text{Hz}, \dots \\ \dots 0.88\text{Hz}, 1.17\text{Hz}, 2.93\text{Hz}, 4.69\text{Hz}, 5.86\text{Hz}.$$

To determine describing functions of linear acceleration and angular velocity channels of the motion cueing algorithm including the motion platform, which is not addressed in Ref. [4], the signals were fed into the respective aircraft linear acceleration and angular velocity inputs of the motion algorithm. Signal amplitude remained constant for all 10 frequencies of a test run. To obtain the describing function of the platform only (covered by Ref. [4]) signals were fed into the direct cabin position path, bypassing the cueing algorithm. During these tests, signal magnitudes were set to fractions of the platform's physical limit at the respective frequency, i.e. magnitude varied with frequency during one test run. FIG 9 visualizes constant and variable magnitude signals used.

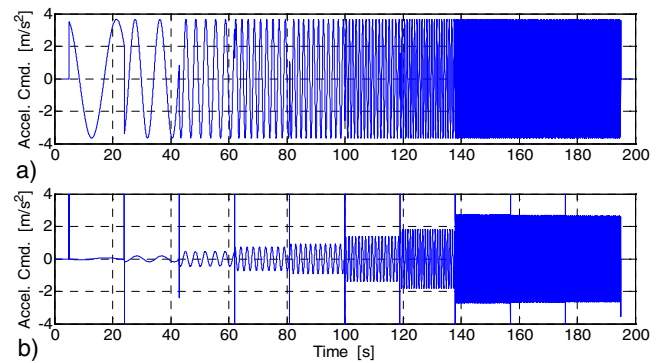


FIG 9: a) Constant amplitude signal used for total system identification; b) variable amplitude signal used for platform identification

Measured acceleration at the pilot's seat as well as linear and angular accelerations at the centroid of the upper actuator joint arrangement, were recorded along with excitation input and supplementary data.

3.1.2. Data Processing

The describing function H at the frequency f_i is the ratio of the Discrete Fourier Transform (DFT) of output signal X_o (measured angular or linear acceleration) and input signal X_i (commanded angular or linear acceleration), both at the fundamental frequency $\frac{k_i}{T}$.

$$(7) H(k_i) = \frac{X_o(k_i)}{X_i(k_i)}.$$

As only linear and angular accelerations can be measured with the installed equipment, direct position and angular rate commands have to be derived before computing the

DFT of the input signal.

The total motion system describing function for one channel comprises the transfer function of the cueing algorithm H_{ca} and the describing function of the motion platform H_p . Combining both yields the total system describing function H_{ca+p} .

$$(8) \quad H_{ca+p} = H_{ca} \cdot H_p .$$

Due to computation time and data transfer, platform reaction will be delayed by the time τ_1 . Hence the effective describing function for platform response to motion command becomes

$$(9) \quad H_{ca+p,eff} = e^{-s\tau_1} \cdot H_{ca} \cdot H_p .$$

Sensor data from the additional accelerometers installed under the pilot's seat are also subject to time delays. In order to determine the time delay τ_2 caused by A/D-conversion and data transfer from test bench to simulation host, a time-based saw-tooth signal is used. As indicated by the dotted line in FIG 8, this reference signal is generated in the host computer and looped through the test bench, before being recorded in the host computer. Delay suffered by the reference signal is twice the delay of pilot seat acceleration measurements τ_2 . FIG 10 shows original and looped reference signal.

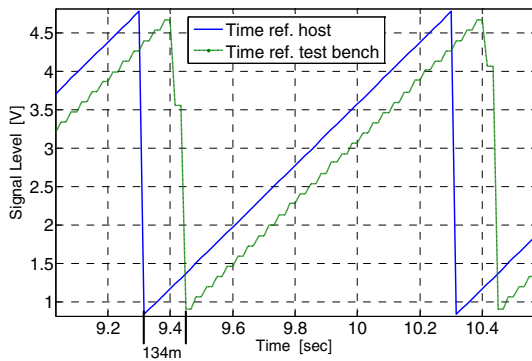


FIG 10. Time reference signals

Cross-correlation of host and loop signal yields an average time delay of 8 host iterations or 134ms. Actual time delay of seat accelerometer data τ_2 follows with

$$\tau_2 = 67\text{ms} .$$

Seat accelerations are corrected for that time delay during post-processing. The 30Hz sample rate of the test bench is also visible in FIG 10.

3.1.3. Test Results

Time delay τ_1 of the motion system command path, plotted as dashed line in FIG 8, was determined measuring platform response to step input signals. The motion-base mounted platform accelerometers were used. The motion computer reads the sensor data and performs jack control with a sample rate of 2000Hz, i.e. practically no noticeable time delay occurs during the read operation. Signal delays

mainly originate from data transfer host→motion computer, during processing in the motion computer and transfer of measurements back to the host. Recorded step response measurements contain both, the time delay caused on the command path host→simulator cabin, as well as the delay on the measurement path sensor→host. The time delay including both paths was determined to be

$$\Delta t = 68\text{ms} .$$

Assuming inflicted time delays are identical on the way from the host and back to the host computer, the command path signal delay follows

$$\tau_1 = \frac{\Delta t}{2} = 34\text{ms} .$$

Computing describing functions H_{ca+p} , as laid out in Eq.(7), the resulting phase has to be corrected for the time delay τ_1 .

FIG 11 gives describing functions H_p for the linear channels of the platform itself; describing functions H_{ca+p} including cueing algorithm and platform are presented in FIG 12.

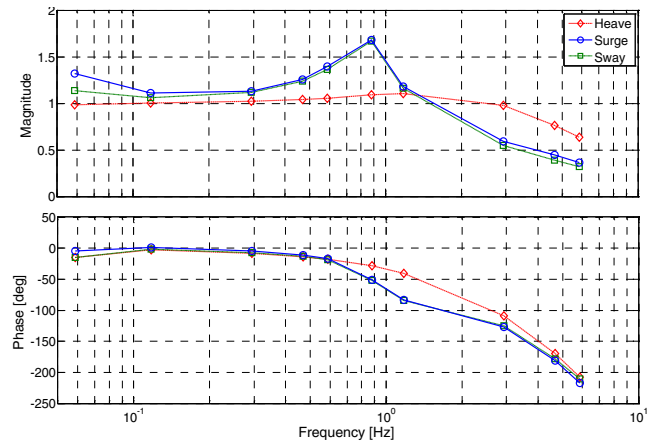


FIG 11: Surge (x-), sway (y-) and heave (z-) describing functions H_p of the motion platform at 10% of system limits

The platform behavior in lateral and longitudinal direction, as depicted in FIG 11, shows significant resonance peaks around the breaking frequency of 0.9Hz. These peaks are also visible in FIG 12. Furthermore FIG 12 shows a low-frequency response in surge and sway axis realized through tilting of the simulator cabin. The describing function displayed for these axes are composed of the high-pass linear and low-pass tilt-coordination transfer behavior, i.e. show transfer behavior of two combined signal paths instead of one path for the heave axis.

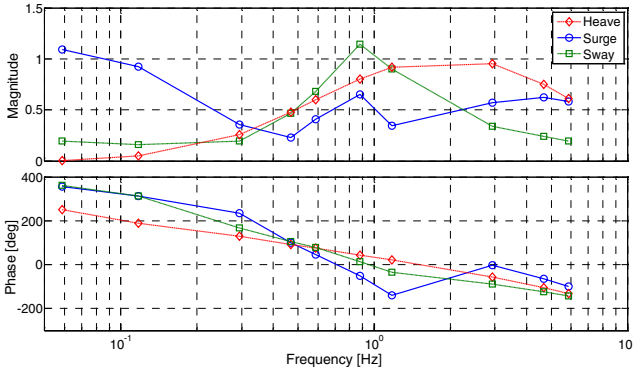


FIG 12: Surge (x), sway (y) and heave (z) describing functions including cueing algorithm H_{ca+p} at 0.12g excitation

As can be seen in FIG 5, the motion cueing algorithm does not allow direct excitation of platform angular position, bypassing the cueing algorithm. Consequently for the angular channels, only the describing function H_{ca+p} , including cueing algorithm and platform, is shown in FIG 13.

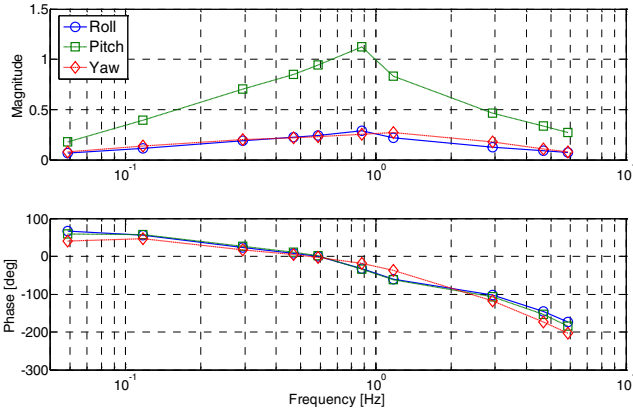


FIG 13: Angular acceleration describing functions H_{ca+p} in roll, pitch and yaw axis. 1.9°/s excitation magnitude

Describing functions of the platform itself will be used as part of a motion system simulation. The describing functions including cueing algorithm will be used to validate this simulation model, which will find primary use for cueing filter adaptation. Simulation based methods to compute the platform's describing functions also for the angular channels will be outlined in the following section.

3.2. Simulation Model of Motion System

To act as an off-line test-bed for cueing parameter tuning as well as parameter estimation of motion platform models, a motion system simulation was developed in Matlab/Simulink. The Simulink model also enables checking of modified motion system response to flight simulation outputs before actual full-flight-simulator testing. Thus, safety of simulator research operation is improved.

The model consists of the following components:

- a reproduction of the motion computer's relevant functions
- the simulation host computer's data recording

functions, motion computer interfaces as well as a function to read real-test excitation signals from disc

- a motion platform model, including sensor models

The system model uses original parameter naming and the data recording format is identical to the test data format.

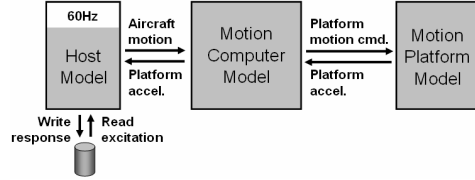


FIG 14: Structure of the motion simulation model

3.2.1. Computation of Angular Channel Platform Describing Functions

In addition to the experimental method of determining platform describing functions, which is not practicable in the angular channels, a simulation based approach has been used. As the simulation model comprises the cueing algorithm, the aforementioned steps to determine a describing function can be applied to the model of the cueing algorithm, yielding H_{ca} . The describing function for cueing algorithm and platform combined H_{ca+p} can be derived from experimental data as shown in FIG 12 and FIG 13.

Solving Eq. (8) for the platform describing function H_p one yields

$$(10) H_p = H_{ca}^{-1} \cdot H_{ca+p}.$$

The results of this method for the angular channels are presented in FIG 15.

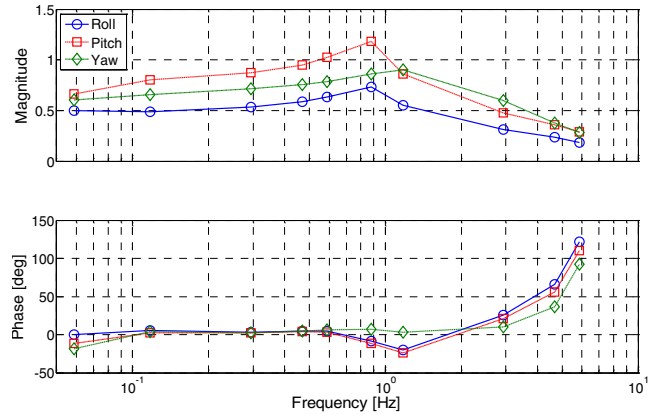


FIG 15: Motion platform describing functions H_p in roll, pitch and yaw axis, identified using motion simulation and angular cueing path measurements. 1.9°/s excitation magnitude.

3.2.2. Estimation of Platform Describing Functions

An alternative approach to determine platform describing functions is to apply parameter estimation methods. Assumptions are made for the platform's linear and angular describing functions. Function parameters are obtained through parameter optimization, using real test excitation signals and matching simulation output to test measurements in time or frequency domain. The approach is outlined in FIG 16. Describing functions found can be used directly for the follow-on task of motion adaptation.

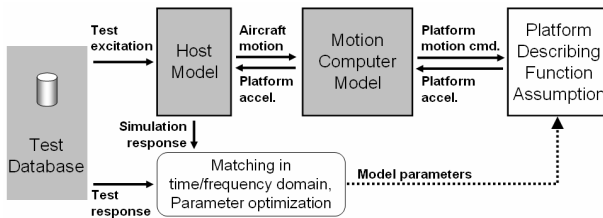


FIG 16: Obtaining platform characteristics by model optimization

4. ADAPTATION OF MOTION SYSTEM CHARACTERISTICS

4.1. Adaptation Goal

Motion cueing algorithms used for training are well optimized to make best use of the platform's motion envelope. For research tasks it can be essential though to reproduce the real flight motion perception, on a limited frequency range, by exact magnitude and phase. For this purpose a deterioration of motion performance outside the frequency interval of interest might be acceptable. Consequently, the goal of the presented approach of modifying cueing parameters is to meet clearly defined requirements in terms of magnitude and phase on a narrow frequency interval. A conceivable requirement for handling quality studies involving flexible transport aircraft would be reaching unity magnitude +/-20% and a phase of +/-45° between 1 and 3Hz in lateral linear (sway) direction.

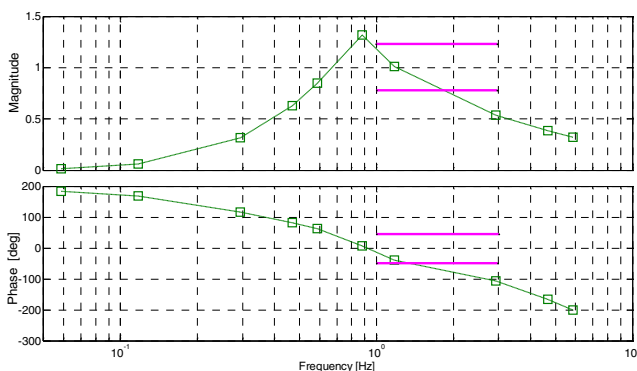


FIG 17: Example for magnitude and phase requirements in sway(y) axis

4.2. Procedure

Based on the status-quo and the adaptation requirements the cueing parameters can be modified to meet test demands in terms of motion characteristic. Changed parameters are entered into the cueing algorithm of the simulation model. Subsequently harmonic input signals from the test database are fed into the system simulation to obtain frequency response data with the modified filter parameters. After meeting the design criteria with the desired accuracy the system simulation tool is used to check if the motion platform remains within allowable bounds of the envelope. The envelope should not be utilized entirely as non-linearities in system behavior become more noticeable for large cabin displacements. Also the motion drive logic features safety functions which retard and limit actuator movement well before reaching physical limits. Therefore the motion envelope should not be utilized to more than 70% of the platform's capabilities. After checking for envelope violation, changed motion filter parameters can be implemented into the simulator's motion computer. FIG 18 further explains the adaptation process.

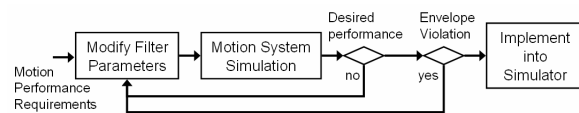


FIG 18: Motion filter adaptation process

Before a new set of filter parameters is used for pilot-in-the-loop studies the success of motion cueing adaptation should be reviewed, i.e. a test run as described in section 3.1 should be conducted in order to determine the complete motion system describing function.

4.3. Results

Neglecting the low-pass tilt-coordination channel which reproduces low-frequency acceleration, the example depicted in FIG 17 uses a high-pass filter of the form

$$H(s) = \frac{s^3}{s^3 + 6s^2 + 10s + 2}$$

without real-time filter gain adaptation. As result of the adaptation process described in the previous section, the following modified high-pass acceleration filter was concluded

$$H(s) = 2.8 \cdot \frac{s^3}{s^3 + 23.31s^2 + 144.03s + 32}$$

FIG 19 compares the experimental sway describing function (DF) for the complete motion system with describing functions obtained by combining the experimental DF for lateral platform motion with the example cueing filter and a modified filter. As can be seen the modified cueing filter meets the set requirements in combination with the motion platform. The describing function computed from test data shows discrepancies in phase and magnitude for low frequencies, as it includes the low-pass tilt-coordination channel.

Adapting one axis to a realistic set of requirements is a fairly quick process. However, in order to serve more intricate demands, also including changes of filter order, real-time gain adaptation or modifications to weighting functions, and to facilitate multi-channel adaptation, a parameter optimization tool should be introduced into the adaptation process.

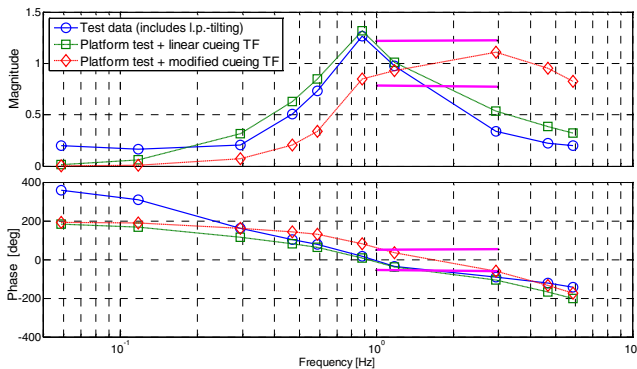


FIG 19: Total system sway describing function (DF), combination of platform DF and linear cueing transfer function (TF), platform DF and modified cueing TF

5. SUMMARY AND OUTLOOK

Characteristics of the simulator motion system (nominal research configuration) have been experimentally determined. The results are used to develop a motion system simulation as well as for model validation. This simulation model serves as a tool for motion system adaptation to the specific demands of pilot-in-the-loop studies, i.e. adjustment of motion characteristics on a limited frequency range. Approaches for the adaptation process have been developed. Preliminary results have been achieved and have to be validated in the Full-Flight-Simulator. The adaptation process will be greatly enhanced by employing an optimization tool for limited automatic cueing algorithm synthesis. The insight gained by the work reported on will assist in materializing such an approach and interpreting its results.

ACKNOWLEDGEMENTS

The work reported here was sub-contracted by Airbus Deutschland GmbH as part of the MODYAS research project (Multi objective dynamic aircraft synthesis, contract No.20A0306), which was funded by the German "Ministerium für Wirtschaft und Technologie (BMW)".

- [1] D.T. McRuer, E.S. Krendel, "Mathematical Models of Human Pilot Behavior," AGARD-AG-188, January 1974
- [2] A.V. Efremov, A.V. Ogloblin, A.N. Predtechensky, V.V. Rodchenko, "Pilot as a Dynamic System", Mashinostroyeniye, Moscow, 1992
- [3] S.K. Advani, "The Kinematic Design of Flight Simulator Motion-Bases," Ph.D. Thesis, Technical University Delft, April 1998
- [4] "Dynamic Characteristics of Flight Simulator Motion Systems," AGARD AR-144, September 1979
- [5] M.A. Mahon, L.D. Reid, J. Kirdeikis, "Adaptive Simulator Motion Software with Supervisory Control," AIAA-90-3133-CP, 1990